Role of MR Imaging and FDG PET/CT in Selection and Follow-up of Patients Treated with Pelvic Exenteration for Gynecologic Malignancies[1]

Yulia Lakhman, MD
Stephanie Nougaret, MD, MSc
Maura Miccò, MD
Chiara Scelzo, MD
Hebert A. Vargas, MD
Ramon E. Sosa, BA
Elizabeth J. Sutton, MD
Dennis S. Chi, MD
Hedvig Hricak, MD, PhD
Evis Sala, MD, PhD, FRCR

Pelvic exenteration (PE) is a radical surgical procedure used for the past 6 decades to treat locally advanced malignant diseases confined to the pelvis, particularly persistent or recurrent gynecologic cancers in the irradiated pelvis. The traditional surgical technique known as total PE consists of resection of all pelvic viscera followed by reconstruction. Depending on the tumor extent, the procedure can be tailored to remove only anterior or posterior structures, including the bladder (anterior exenteration) or rectum (posterior exenteration). Conversely, more extended pelvic resection can be performed if the pelvic sidewall is invaded by cancer. Preoperative imaging evaluation with magnetic resonance (MR) imaging and fluorine 18 fluorodeoxyglucose (FDG) positron emission tomography/computed tomography (PET/CT) is central to establishing tumor resectability and therefore patient eligibility for the procedure. These imaging modalities complement each other in diagnosis of tumor recurrence and differentiation of persistent disease from posttreatment changes. MR imaging can accurately demonstrate local tumor extent and show adjacent organ invasion. FDG PET/CT is useful in excluding nodal and distant metastases. In addition, FDG PET/CT metrics may serve as predictive biomarkers for overall and disease-free survival. This pictorial review describes different types of exenterative surgical procedures and illustrates the central role of imaging in accurate patient selection, treatment planning, and postsurgical surveillance.

Abbreviations: CRT = chemoradiotherapy, DW = diffusion weighted, FDG = fluorodeoxyglucose, FSE = fast spin-echo, LEER = laterally extended endopelvic resection, PE = pelvic exenteration, VRAM = vertical rectus abdominis myocutaneous

RadioGraphics 2015; 35:1295–1313

Published online 10.1148/rg.2015140313

Content Codes: MR NM OB OI

[1]From the Department of Radiology (Y.L., S.N., H.A.V., R.E.S., E.J.S., H.H., E.S.) and Department of Surgery, Gynecology Service (D.S.C.), Memorial Sloan Kettering Cancer Center, 300 E 66th St, Room 703, New York, NY 10065; Department of Bioimaging and Radiological Science, Catholic University A. Gemelli Hospital, Rome, Italy (M.M.); and Department of Surgery, Gynecology and Obstetrics Section, Tor Vergata University, Rome, Italy (C.S.). Presented as an education exhibit at the 2013 RSNA Annual Meeting. Received November 1, 2014; revision requested January 5, 2015, and received January 30; accepted February 12. For this journal-based SA-CME activity, the authors, editor, and reviewers have disclosed no relevant relationships. **Address correspondence to** Y.L. (e-mail: *lakhmany@mskcc.org*).

See also the article by Sagebiel et al in this issue.

SA-CME LEARNING OBJECTIVES

After completing this journal-based SA-CME activity, participants will be able to:

- Describe the indications for and types of PE in women with treatment-resistant primary or recurrent gynecologic malignancies.
- Discuss the use of MR imaging and FDG PET/CT to determine patients' eligibility for PE and provide the surgeon with a preoperative road map for treatment planning.
- Recognize the expected imaging appearance after PE and postsurgical complications.

See www.rsna.org/education/search/RG.

Introduction

Pelvic exenteration (PE) refers to radical en-bloc resection of all pelvic organs affected by cancer followed by pelvic reconstruction to reestablish abolished vital bodily functions (1). At the time of its description by Alexander Brunschwig in 1948, PE was a palliative procedure intended for relief of symptoms caused by advanced pelvic malignancies uncontrolled by radiation therapy (2). Due to steady advances in reconstructive surgical techniques and improvements in perioperative management, exenterative surgery has quickly evolved from a purely palliative approach to a potentially curative operation with over 50% 5-year survival in carefully selected patients with treatment-resistant tumors confined to the pelvis (3,4). Gynecologic cancers constitute the most common indication for PE and are the focus of this review.

PE is a major undertaking for both patients and their physicians. Although surgery-related mortality is now less than 5%, the rate of severe postoperative complications still exceeds 50% (1). Therefore, careful preoperative patient evaluation is essential to select only those patients who will benefit from this operation. Until recently,

TEACHING POINTS

- Recently published data suggests that the cornerstones of long-term survival after salvage (curative intent) PE (regardless of exact exenterative procedure type) are the absence of nodal and systemic metastases at preoperative evaluation and negative histopathologic margins at excision.
- At our institution, the absolute contraindications for PE with curative intent are *(a)* distant metastases and *(b)* peritoneal disease. The relative contraindications vary and are greatly influenced by the local surgical expertise. However, commonly accepted relative contraindications include *(a)* nodal metastases and *(b)* tumor encasement of the common or external iliac vessels or involvement of the sciatic nerve or lumbosacral plexus, since these situations usually preclude R0 resection.
- Pelvic MR imaging is useful for diagnosis of persistent or recurrent tumor and differentiation between active disease and post–radiation therapy changes. Furthermore, it is essential for evaluation of tumor extent to predict the likelihood of complete excision, tailor the magnitude of the operation, and anticipate the need for a multidisciplinary surgical team approach. FDG PET/CT is helpful in making the distinction between tumor recurrence and radiation-induced changes, as well as detection of nodal or systemic metastases.
- In oncologic patients, FDG avidity at FDG PET/CT can indicate active disease, but it may also be physiologic in etiology or related to posttreatment inflammation, infections, or radiation-induced fistulas or insufficiency fractures.
- Most recurrences occur within 2 years of PE; the majority manifest as a pelvic mass or retroperitoneal or inguinal lymphadenopathy. New asymmetric soft tissue or enhancement at CT or MR imaging should be regarded with suspicion. MR imaging may be better than CT for detection of recurrent disease due to its superior soft-tissue contrast. FDG PET/CT may also help identify disease recurrence by demonstrating hypermetabolic tumor or lymphadenopathy.

exploratory laparotomy or diagnostic laparoscopy was considered a necessary part of preoperative assessment. This surgical "go-and-see" approach was eventually called into question due to the increasing availability and validation of imaging. Magnetic resonance (MR) imaging and fluorine 18 fluorodeoxyglucose (FDG) positron emission tomography/computed tomography (PET/CT) now play a central role in presurgical evaluation (1,5). After exenterative surgery, cross-sectional imaging is important for detection of postoperative complications and disease recurrence.

In this article we highlight different types of PE and approaches for pelvic reconstruction. We also review how MR imaging and FDG PET/CT serve as a preoperative road map for treatment planning. In addition, we describe how MR imaging and FDG PET/CT help distinguish persistent or recurrent tumors from post–radiation therapy changes, and illustrate how to avoid potential pitfalls caused by prior radiation therapy. Finally, we review the expected posttreatment appearance of the pelvis and common complications after PE.

Pelvic Exenteration

Types of PE

PE may consist of complete PE (ie, total exenteration) or partial PE (ie, anterior or posterior exenteration), depending on the location and extent of the tumor. Total PE involves resection of the female reproductive organs, lower urinary tract, rectosigmoid colon, anus, and surrounding soft tissues (Fig 1a). In anterior exenteration, the rectum and anus are spared from resection (Fig 1b), while in posterior exenteration the urinary bladder and urethra are preserved (Fig 1c). PE is further classified into supralevator or infralevator (translevator) resection (5). In supralevator exenteration, pelvic viscera are divided above the pelvic floor muscles preserving the levator ani muscles, anal sphincter, and urogenital diaphragm. In infralevator exenteration these structures are resected (5).

Conventional exenterative techniques are suitable only for patients with central pelvic tumors because complete removal of all disease with microscopically negative margins (R0 resection) can be achieved only for these masses (1). Traditionally, pelvic sidewall disease has been a contradiction to PE, as tumor-free margins could not be achieved and oncologic outcome was poor. Laterally extended endopelvic resection (LEER) and extended pelvic resection (EPR) are procedures that have been introduced to address this limitation (6–8). LEER is laterally extended excision of any of the following sidewall structures: pelvic sidewall fat, internal iliac vessels, obturator internus muscles, and levator ani muscles. This procedure is best suited for tumors situated below the major pelvic vasculature (ie, common and external iliac vessels) and remote from the lumbosacral plexus, sciatic, and obturator nerves (1,8). EPR is an ultraradical procedure defined as en bloc resection of a pelvic tumor along with pelvic sidewall muscles (obturator internus, iliacus, and/or psoas muscles), a portion of the pelvic bones, and major neural and/or major vascular structures (6,7).

Pelvic Reconstruction

Pelvic reconstruction is an integral part of PE in part because dead space (ie, unfilled space left in the body after extensive resection) and radiation-related tissue ischemia may result in high postsurgical morbidity. Thus, the goals of the reconstruction are to reestablish one or more compromised bodily functions, decrease dead space, restore structural support to the pelvic organs, ensure adequate wound closure and healing, and promote normal sexual function and body image (9).

Surgeons have many choices for pelvic reconstruction and individualize procedures to best

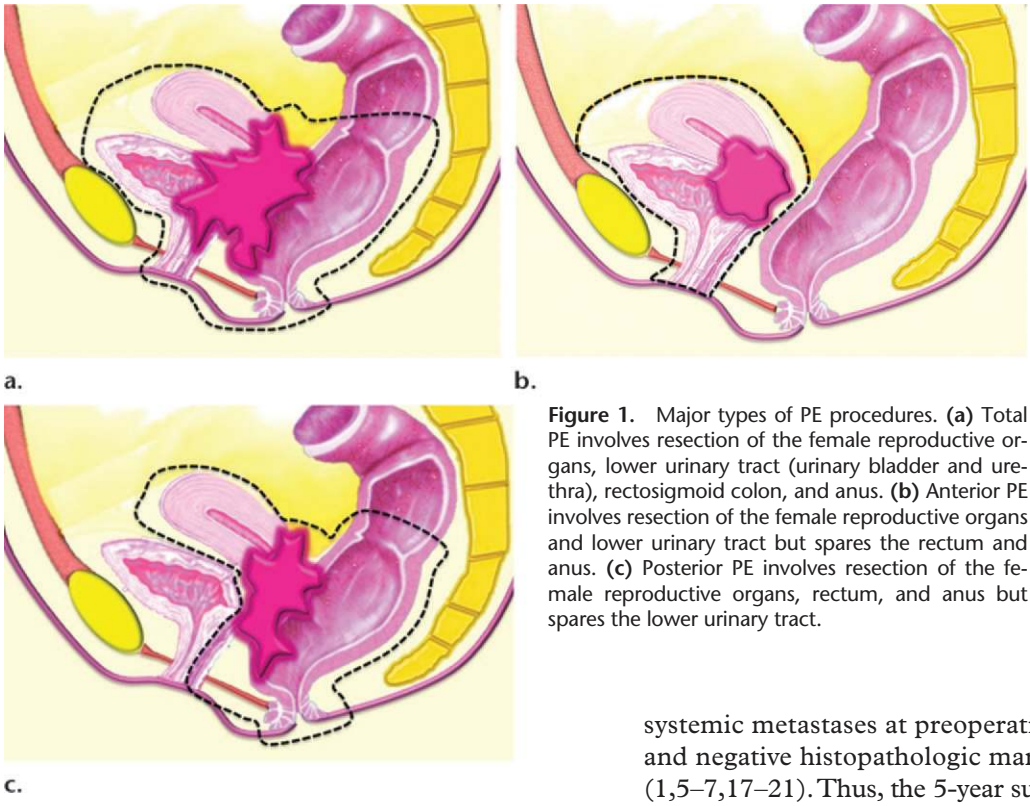

Figure 1. Major types of PE procedures. **(a)** Total PE involves resection of the female reproductive organs, lower urinary tract (urinary bladder and urethra), rectosigmoid colon, and anus. **(b)** Anterior PE involves resection of the female reproductive organs and lower urinary tract but spares the rectum and anus. **(c)** Posterior PE involves resection of the female reproductive organs, rectum, and anus but spares the lower urinary tract.

address each patient's needs. Surgical techniques to reestablish urinary function include creation of a noncontinent urinary diversion (such as an ileal conduit), continent pouch, or orthotopic neobladder (1,5,10–12). The type of exenteration performed influences the need for anorectal reconstruction. If the anal sphincter is sacrificed in the course of translevator exenteration, the bowel function is substituted via a permanent endcolostomy. If the anal sphincter is preserved with a supralevator exenteration, coloanal anastomosis is an option (11,13). Possible reconstruction methods for vaginal, peritoneal, and pelvic floor reconstruction include omental pedicle flap (Fig 2a–2c), vertical rectus abdominis myocutaneous (VRAM) flap, Singapore (or pudendal thigh) fasciocutaneous flap, or bilateral gracilis myocutaneous flaps (Fig 2d, 2e) (9,11,14–16).

Indications and Contraindications for PE

PE is most commonly performed in patients with treatment-resistant cervical cancer after primary chemoradiotherapy (CRT) or surgery with adjuvant CRT. Other frequent indications are recurrent endometrial, vaginal, and vulvar cancers after radiation or CRT (1).

Recently published data suggests that the cornerstones of long-term survival after salvage (curative intent) PE (regardless of exact exenterative procedure type) are the absence of nodal and systemic metastases at preoperative evaluation and negative histopathologic margins at excision (1,5–7,17–21). Thus, the 5-year survival rate is around 50% for patients with negative margins but declines to less than 10% when the margins are positive (1,20). Similarly, N1 disease reduces the 5-year survival rate from 47% to 23% (1).

At our institution, the absolute contraindications for PE with curative intent are *(a)* distant metastases and *(b)* peritoneal disease. The relative contraindications vary and are greatly influenced by the local surgical expertise. However, commonly accepted relative contraindications include *(a)* nodal metastases and *(b)* tumor encasement of the common or external iliac vessels or involvement of the sciatic nerve or lumbosacral plexus, since these situations usually preclude R0 resection. Other variables that may influence the decision to proceed with surgery are the patient's functional status, duration of disease-free interval, and tumor size.

Preoperative Imaging Evaluation

Preoperative pelvic MR imaging and FDG PET/CT are now an integral and critical part of comprehensive patient evaluation before surgery. Pelvic MR imaging is useful for diagnosis of persistent or recurrent tumors and differentiation between active disease and postradiation changes. Furthermore, it is essential for evaluation of tumor extent to predict the likelihood of complete excision, tailor the magnitude of the operation, and anticipate the need for a multidisciplinary surgical team approach (22–27). FDG PET/CT is helpful in making the distinction between tumor recurrence and radiation-induced

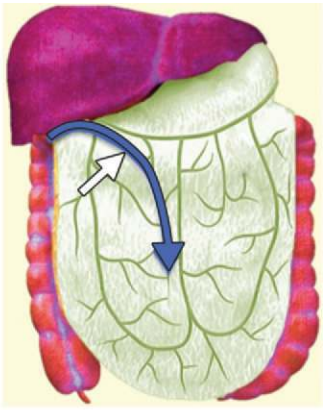

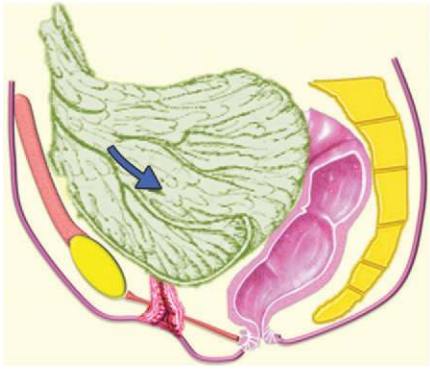

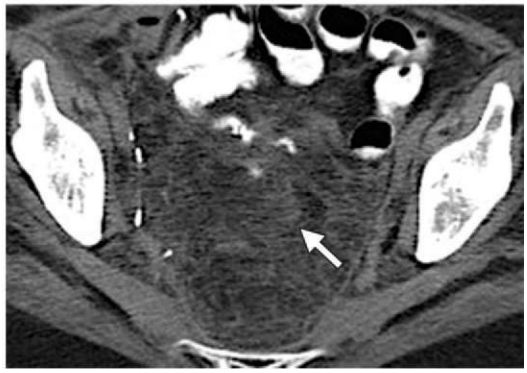

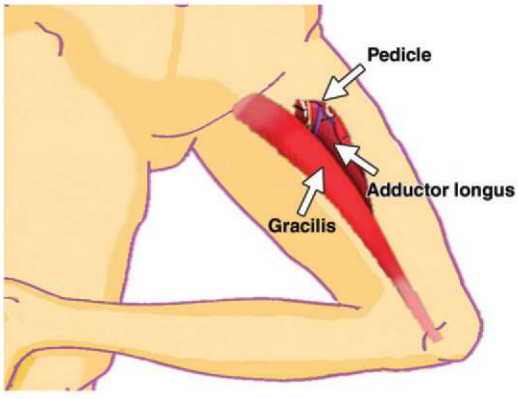

Figure 2. **(a)** Drawing shows the anatomy of the omental pedicle flap. Greater omentum, composed largely of fat and lymph nodes, is used for omental pedicle flaps. The greater omentum hangs down from the greater curvature of the stomach and is supplied by the right and left gastroepiploic arteries. The vascular supply of the omental flap is based on the arterial arcades arising from the right or left gastroepiploic arteries (blue and white arrows = dissection plane from the right gastroepiploic artery). The flap is dissected from the greater curvature of the stomach and the transverse colon, tunneled via one of the paracolic gutters, and placed into the pelvis (blue arrow). **(b)** Drawing shows an omental pedicle flap (blue arrow) filling pelvic dead space created by the surgical resection. **(c)** Unenhanced axial CT image, obtained in a 63-year-old patient with recurrent cervical carcinoma who underwent total PE and pelvic reconstruction, shows an omental pedicle flap, evident as prominent fatty tissue in the pelvis (arrow). **(d)** Drawing shows the anatomy of the gracilis myocutaneous flap. The vascular supply of the gracilis flap is derived from the medial femoral circumflex artery. First, the skin is incised and the gracilis muscle is exposed, then the main vascular pedicle is identified and preserved. After the proximal and distal muscle attachments are divided, the flap is tunneled through the subcutaneous skin into the vaginal defect and brought out through the introitus. The bilateral flaps are sutured to each other in the midline. The neovagina is shaped into a pouch and then inserted into the pelvic space that is left after the exenteration. The proximal end of the neovagina is sutured to the introitus. **(e)** Contrast-enhanced axial CT image obtained in a 60-year-old patient with recurrent cervical carcinoma who underwent anterior PE shows vaginal reconstruction with bilateral gracilis myocutaneous flaps (white arrows). The small amount of air in the neovagina (black arrow) is a normal imaging finding.

changes, as well as detection of nodal or systemic metastases (28). Furthermore, quantitative FDG PET/CT–derived metrics such as metabolic tumor volume (MTV) and total lesion glycolysis (TLG) may serve as predictive biomarkers for recurrence-free and overall survival (29).

MR Imaging Technique

Our standard MR imaging protocol for workup of known or suspected persistent or recurrent gynecologic cancer is summarized in the Table. High–spatial resolution small–field of view multiplanar T2-weighted FSE imaging is crucial for detecting the tumor and evaluating its relationship to the adjacent pelvic organs. The exact site of disease determines the choice of the optimal imaging planes. The addition of fat saturation to T2-weighted sequences is useful in patients with vulvar cancer to improve tumor conspicuity (30). We routinely incorporate DW MR imaging into our imaging protocol, as it may improve the conspicuity of the pelvic tumor, regional metastases, and peritoneal deposits (27). Figure 3 summarizes the key points that should be included in the MR imaging report.

FDG PET/CT Protocol

FDG PET/CT is a noninvasive functional imaging technique that combines metabolic PET data with anatomic CT information. At our institution, patients fast for at least 6 hours to ensure that the serum glucose concentration is less than 200 mg/dL before intravenous FDG injection. Oral contrast

MR Imaging Protocol at 3 T for Workup of Known or Suspected Persistent or Recurrent Gynecologic Cancer

	Imaging Sequence						
Parameters	Axial T1W	Sagittal T2W	Axial T2W	Coronal T2W	Axial Abdominal T2W	Axial DW*	Axial Multiphase DCE†
Sequence type	FSE	FRFSE	FRFSE	FRFSE	FRFSE-RT FS	EPI	3D GRE
Imaging time							
Echo time (msec)	Minimum	85–100	85–100	85–100	85–102	Minimum	Minimum
No. of signals acquired	2	4	4	4	2	16	1
Repetition time (msec)	470	3500	3500	3500	Per respiratory rate	5000	Default
Bandwidth (kHz)	62	62	62	62	83	…	62
Echo train length	2	23–25	23–25	23–25	13	…	…
Imaging range							
Field of view (cm)	28	20–24	20–24	20–24	28–36	28	28
Section thickness (mm)	5	4	4	4	7	4	4
Gap (mm)	1	1	1	1	1	0	−2
Flip angle (degrees)	90	90	90	90	90	…	12
Phase-encoding steps	288	256	256	256	256	128	192
Frequency steps	448	512	512	512	320	128	320
Phase direction	RL	SI	RL	RL	AP	AP	AP

Note.—AP = anterior-posterior, DCE = dynamic contrast-enhanced, DW = diffusion-weighted, EPI = echo-planar imaging, FRFSE = fast-recovery FSE, FRFSE-RT = FRFSE with respiratory triggering, FS = fat-saturated, FSE = fast spin-echo, GRE = gradient-echo, RL = right-left, SI = superior-inferior, 3D = three-dimensional, T1W = T1-weighted, T2W = T2-weighted.

*b value = 800 sec/mm^2.

†Timing relative to intravenous administration of contrast material: before injection and 1, 2, and 3 minutes after injection.

material is routinely given, while intravenous iodinated contrast material is administered only if performance of diagnostic PET/CT is desired (31). To limit the intense physiologic FDG activity in the urinary bladder, patients are asked to void before image acquisition. Some institutions mandate urinary bladder catheterization, while other centers ask patients to empty their bladder after the initial whole-body PET acquisition and, in addition, obtain postvoiding images through the pelvis.

Attenuation correction with CT data used in FDG PET/CT may lead to artifacts when photopenic areas corresponding to high-attenuation structures at CT (eg, brachytherapy seeds) appear falsely FDG avid on attenuation-corrected PET images (Fig 4) (31). When interpreting FDG PET/CT images, radiologists should be aware of this overcorrection artifact on attenuation-corrected PET images.

Detection of Tumor Recurrence

As noted earlier, treatment-resistant cervical cancer is the most common indication for PE. In patients with advanced cervical cancer who are treated with primary CRT, MR imaging is used to evaluate the response during and after treatment (32). The traditional approach relies on the change in tumor size between sequential MR imaging examinations. Tumor shrinkage can be seen as early as 2 months after CRT and is indicative of a good prognosis (33). Reconstitution of the normal low-signal-intensity cervical stroma after radiation therapy is the most reliable predictor of a tumor-free cervix, with a negative predictive value of 97% (Fig 5a, 5c) (34,35).

DW MR imaging and dynamic contrast-enhanced MR imaging may complement this standard morphologic response assessment based on tumor size (Fig 5) (27). Posttherapy FDG uptake is also a useful tool to monitor the response to CRT or radiation therapy. Three-month post-therapy FDG PET acts as a prognostic biomarker, with 3-year overall survival rates of 78%, 33%, and 0% in patients with complete metabolic response, partial metabolic response, and progressive disease at 3 months, respectively (36). If MR imaging and FDG PET/CT demonstrate small residual tumor at the completion of therapy, there is a window of opportunity to offer exenterative surgery.

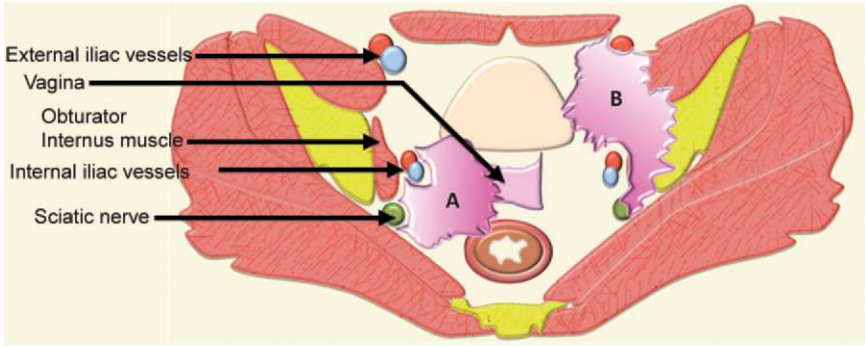

Figure 3. Key points that should be part of the MR imaging report. A comprehensive report should describe the presence, location, and size of the tumor. It should inform regarding the probability of urinary bladder, urethral, rectal, anal, and pelvic sidewall invasion (illustrated by tumor *A*). It should state the likelihood of vascular (common and external iliac) and neural (lumbosacral plexus and sciatic nerve) involvement (illustrated by tumor *B*). Potential contraindications to the surgery such as vascular or neural encasement and bone invasion (illustrated by tumor *B*) should be stated. In addition, the presence of lymphadenopathy, peritoneal implants, and distant metastases should be described in the imaging report.

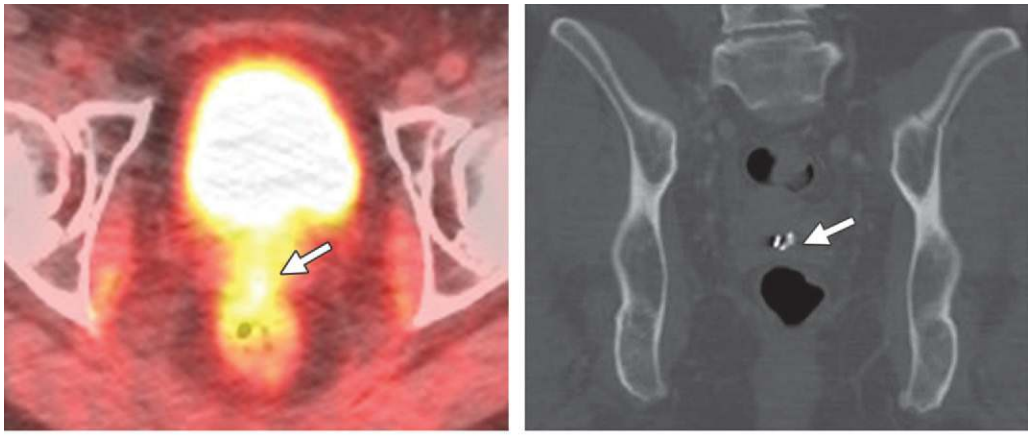

a. b.

Figure 4. Overcorrection artifact in a 40-year-old patient with cervical carcinoma treated with CRT. **(a)** Axial FDG PET/CT image shows a hypermetabolic focus in the vaginal vault (arrow). **(b)** Coronal CT image shows a cluster of brachytherapy seeds (arrow) corresponding to the hypermetabolic region in **a**.

Cervical cancer generally recurs within the first 2 years of the initial treatment (37). Recurrence is defined as development of active disease after a disease-free interval of at least 6 months. At MR imaging, recurrent tumor may be differentiated from radiation-induced fibrosis on the basis of its signal intensity on T2-weighted images. Fibrosis typically has low signal intensity on both T1- and T2-weighted images, whereas tumor has intermediate to high T2 signal intensity (Fig 5e) (27). However, the appearance on T2-weighted images can be indeterminate, particularly in the first 6 months after radiation therapy, as acute radiation-induced edema and inflammation are both typically T2 hyperintense (38).

The diagnostic performance of MR imaging may be improved by addition of dynamic contrast-enhanced and DW MR sequences. Recurrent tumor usually shows early enhancement on dynamic contrast-enhanced images, while radiation-induced fibrosis demonstrates mild delayed enhancement (24). However, post–radiation therapy edema and inflammation may also enhance, mimicking tumor. At DW MR imaging, hyperintense signal on high-*b*-value images and corresponding low signal on apparent diffusion coefficient (ADC) maps are a hallmark of active disease (Fig 5f) (39). A recent meta-analysis found that the pooled sensitivity and specificity of MR imaging in cervical cancer recurrence are 82%–100% and 78%–100%, respectively (Fig 6) (40). Likewise, FDG PET/CT is useful for restaging cervical cancer. The pooled sensitivity and specificity of FDG PET or FDG PET/CT for assessment of locoregional recurrence are 82% and 98%, respectively (Fig 6) (41).

Another frequent indication for PE is treatment-resistant endometrial carcinoma. Most patients are cured by the primary treatment, and

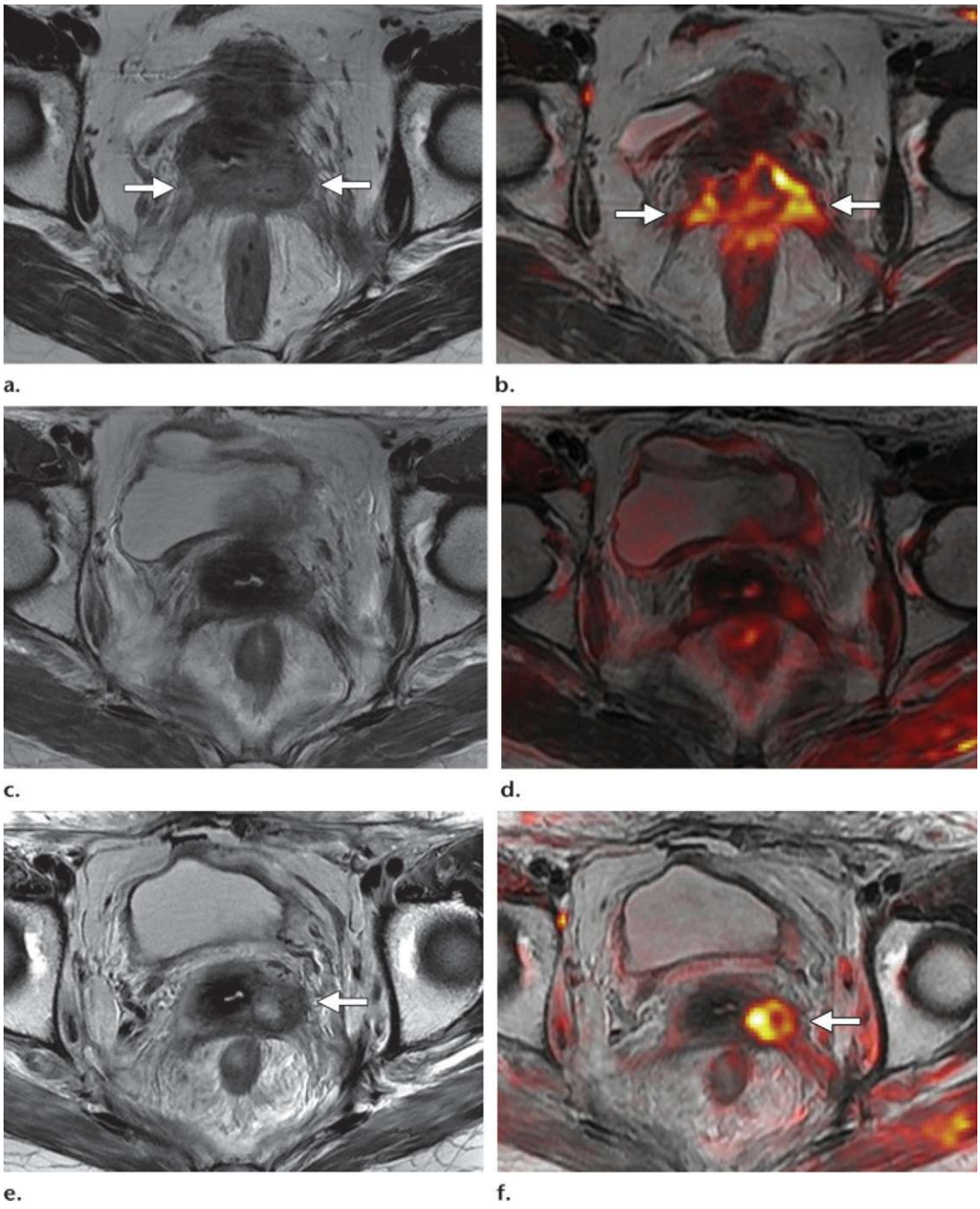

Figure 5. MR imaging evaluation of treatment response in a 55-year-old patient with squamous cell carcinoma of the cervix treated with CRT. **(a, b)** Pretreatment axial FSE T2-weighted **(a)** and fused T2-weighted and DW **(b)** images show a large mildly T2-hyperintense cervical tumor (arrows) with parametrial extension and restricted diffusion. **(c, d)** Axial FSE T2-weighted **(c)** and fused T2-weighted and DW **(d)** images obtained shortly after completion of CRT show reconstitution of the low-signal-intensity cervical stroma and resolution of the restricted diffusion. **(e, f)** Axial FSE T2-weighted **(e)** and fused T2-weighted and DW **(f)** images obtained 7 months after CRT show mildly T2-hyperintense recurrent tumor with restricted diffusion (arrow). (Case courtesy of Shinya Fujii, MD, PhD, Tottori University, Tottori, Japan.)

only 15% of patients with endometrial cancer develop recurrent disease (42). Most recurrences occur within the first 3 years after initial treatment and commonly involve lymph nodes (46%) and the vaginal cuff (42%). The vaginal cuff is the sole site of disease in 30%–50% of endometrial cancer recurrences (43). On T2-weighted images, a recurrent tumor appears as a mass that obliterates the linear low signal intensity of the vaginal cuff, and demonstrates signal intensity similar to that of the primary tumor (27).

Tumor size should be carefully measured in three orthogonal planes and included in the imaging report, since some investigators believe that

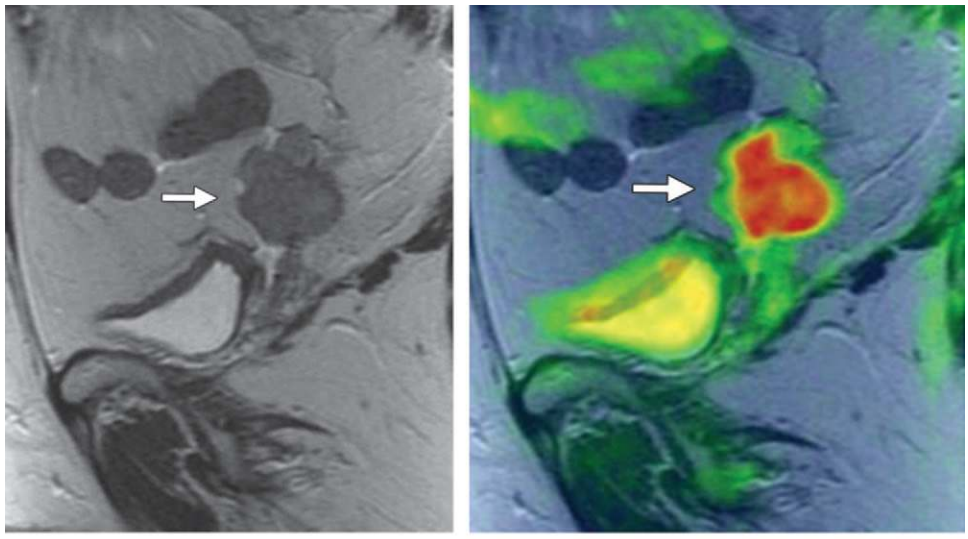

a. b.

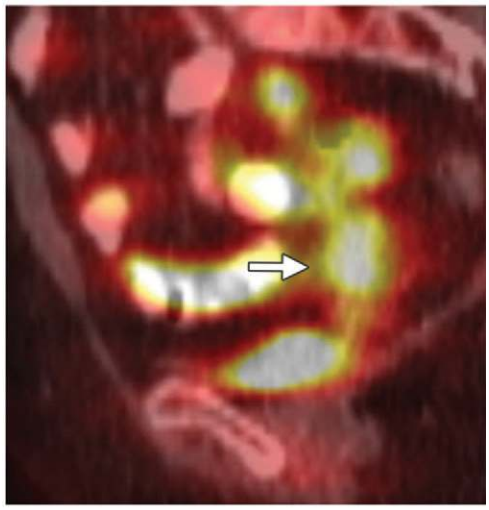

c.

Figure 6. Recurrent cervical carcinoma after radical hysterectomy in a 60-year-old patient. **(a, b)** Sagittal FSE T2-weighted **(a)** and fused T2-weighted and DW **(b)** images show a mildly T2-hyperintense mass with restricted diffusion (arrow) immediately superior to the vaginal cuff. **(c)** Sagittal FDG PET/CT image shows hypermetabolic recurrent tumor (arrow).

tumors greater than or equal to 5 cm are associated with poor patient survival (1).

Assessment of Tumor Extent and Eligibility for PE

Urinary Bladder and Rectum

Accurate detection of urinary bladder and rectal involvement has important implications for the patient's postoperative quality of life. When appropriate, anterior or posterior exenteration may be performed instead of total exenteration, obviating the requirement for a urostomy or colostomy (Fig 1b, 1c). MR images should be carefully scrutinized to determine if the tumor invades either structure, and the imaging report should reflect the radiologist's impression and level of certainty about the likelihood of invasion (Figs 3, 7).

High-resolution small–field of view sagittal and axial oblique T2-weighted images are ideal for assessment of bladder or rectal involvement (26). A clearly defined and uninterrupted fat plane between the tumor and either organ excludes invasion (Fig 7a). On T2-weighted images, bladder or rectal involvement is diagnosed when *(a)* tumor abuts or indents the bladder or rectum over a significant area (probable serosal involvement) (Figs 7b, 8), *(b)* tumor interrupts the low signal intensity of the bladder or rectal muscular layer (probable muscle invasion) (Fig 7c), or *(c)* tumor invades the bladder or rectal muscular wall and tumor nodules are seen in the mucosal layer (mucosal involvement) (Figs 7d, 9) (23,26).

Bullous edema of the bladder, which appears as prominent high-signal-intensity mucosa on T2-weighted images, is a frequent sign of tumor in the subserosal or muscular layer (Figs 7e, 10). However, this sign by itself is insufficient to diagnose bladder invasion, since it can also be seen with acute cystitis from any etiology, including recent radiation therapy.

Using these imaging criteria, MR imaging has high positive predictive value (up to 100%), high negative predictive value (up to 90%), and high accuracy (up to 95%) for assessment of bladder and rectal wall involvement in patients undergoing PE (23,25). At FDG PET/CT, bladder and rectal invasion is suspected when there is no fat plane between an FDG-avid tumor and either organ in the CT component of the study (29), although accurate evaluation of bladder invasion can be hin-

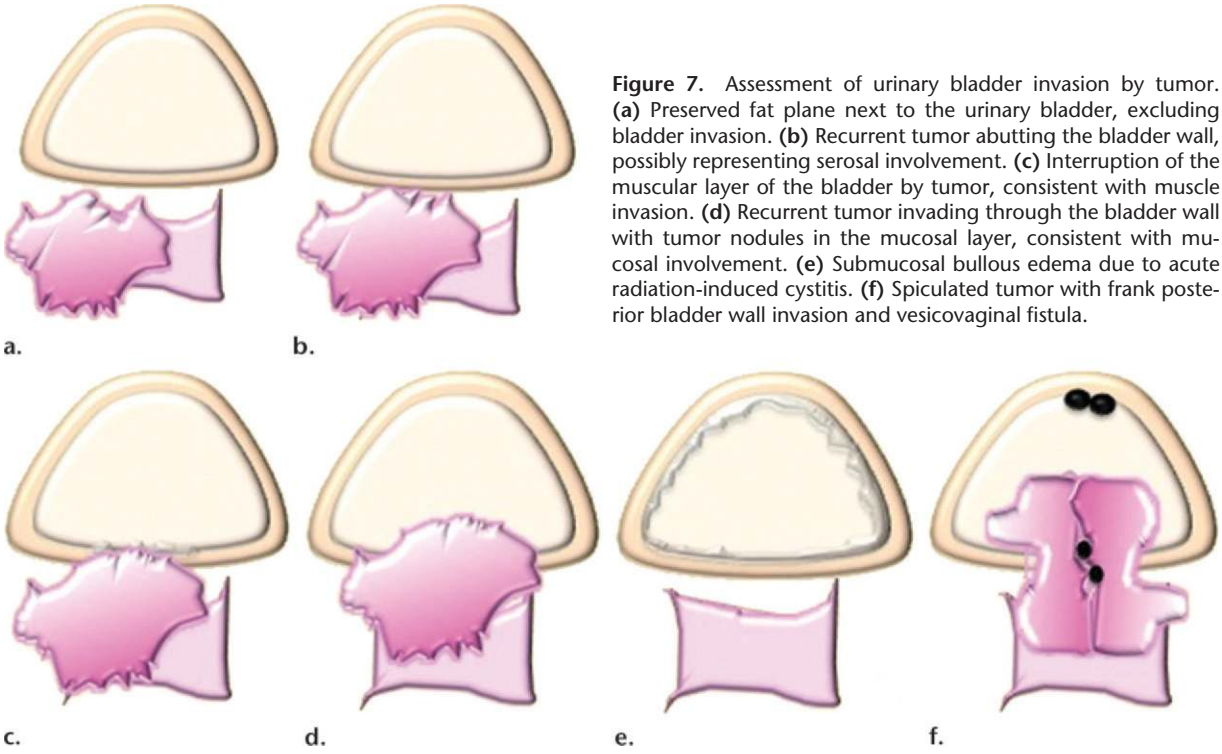

Figure 7. Assessment of urinary bladder invasion by tumor. **(a)** Preserved fat plane next to the urinary bladder, excluding bladder invasion. **(b)** Recurrent tumor abutting the bladder wall, possibly representing serosal involvement. **(c)** Interruption of the muscular layer of the bladder by tumor, consistent with muscle invasion. **(d)** Recurrent tumor invading through the bladder wall with tumor nodules in the mucosal layer, consistent with mucosal involvement. **(e)** Submucosal bullous edema due to acute radiation-induced cystitis. **(f)** Spiculated tumor with frank posterior bladder wall invasion and vesicovaginal fistula.

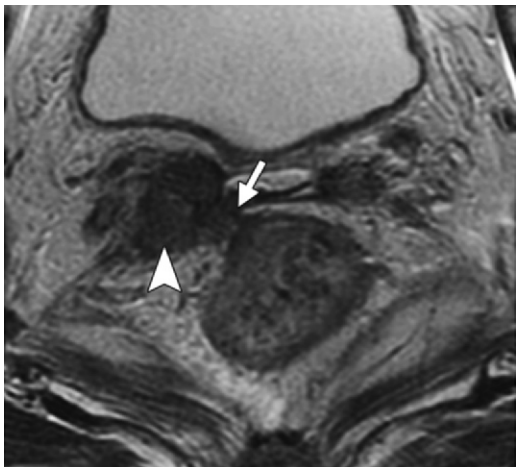

Figure 8. Recurrent cervical carcinoma in a 65-year-old patient. Axial FSE T2-weighted image shows recurrent tumor in the right vaginal cuff (arrowhead) that extends to the rectal serosa (arrow).

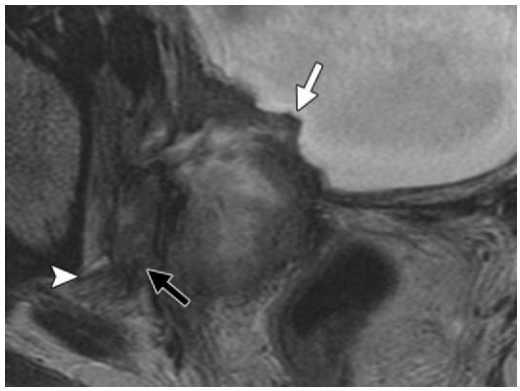

Figure 9. Recurrent cervical carcinoma in a 57-year-old patient. Axial FSE T2-weighted image shows a large recurrent tumor invading through the urinary bladder muscle wall into the mucosa (white arrow), consistent with mucosal involvement. Note the encasement and distortion of the right sciatic nerve (arrowhead) by tumor (black arrow).

dered by the presence of physiologically excreted tracer in the bladder lumen.

Urethra

Urethral involvement by persistent or recurrent tumor necessitates translevator exenteration with resection of the urogenital diaphragm. The female urethra is a short tubular conduit, which courses anteroinferiorly from the bladder base and internal urethral meatus to the external urethral meatus (44). It is composed of two concentric layers of smooth muscle that are reinforced by a striated muscle sphincter. On axial and sagittal T2-weighted MR images, the urethra has a low-signal-intensity bull's-eye or concentric ringed appearance, which is disrupted when invaded by tumor (Fig 11).

Anal Sphincter

Information about the involvement of the anal sphincter may influence the magnitude of the resection. If disease spares the anal sphincter, less extensive supralevator exenteration is a possibility. The anal sphincter is composed of the internal sphincter and the external sphincter complex, best assessed on high-resolution coronal and axial T2-weighted images. The internal

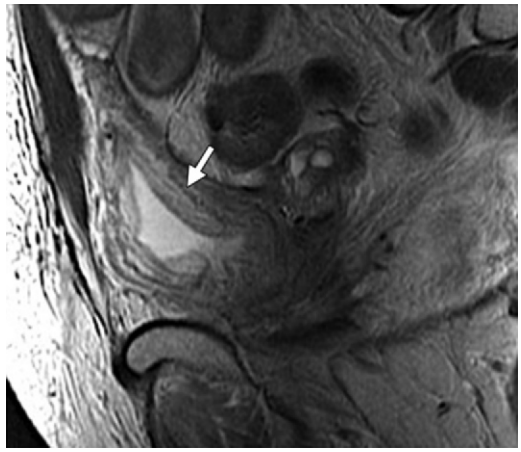

Figure 10. Bullous edema in a 56-year-old patient with cervical carcinoma treated with radical hysterectomy and radiation therapy. Sagittal FSE T2-weighted image shows prominent high-signal-intensity mucosa (arrow), consistent with bullous edema in the setting of acute radiation-induced cystitis.

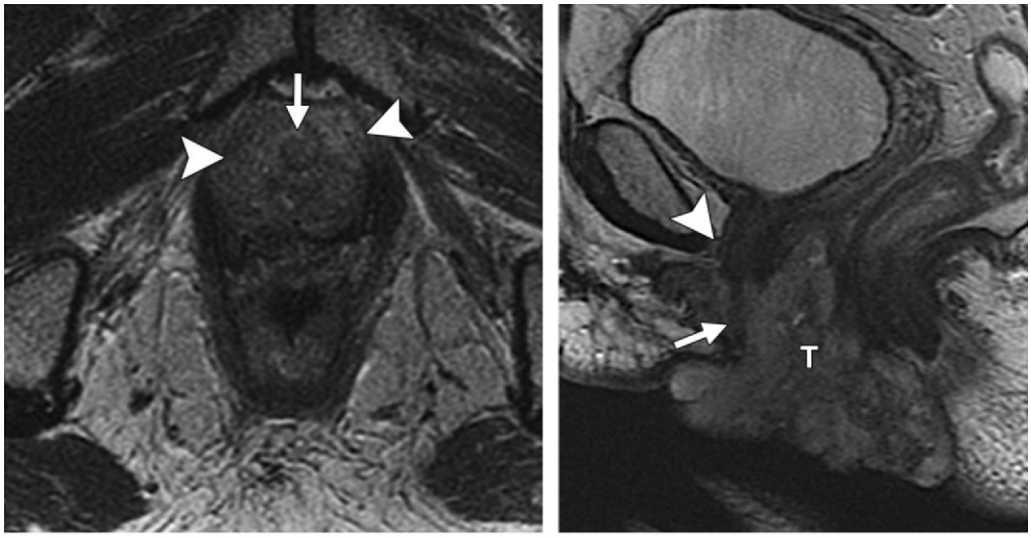

a. b.

Figure 11. Recurrent cervical carcinoma. **(a)** Axial FSE T2-weighted image obtained in a 50-year-old patient shows infiltrative recurrent tumor (arrowheads) encasing the urethra and disrupting its concentric ringed appearance (arrow). **(b)** Sagittal FSE T2-weighted image obtained in a 54-year-old patient shows bulky tumor *(T)* encompassing the vagina, vulva, and perineum and invading the lower urethra (arrow). Note the normal tubular appearance of the upper mid urethra (arrowhead).

sphincter is a continuation of the circular muscle layer of the rectum, which thickens at the anorectal junction.

The external sphincter complex is composed of the inferior portion of the levator ani and the puborectalis muscles. The superior margin of the puborectal sling forms the upper edge of the surgical anal canal. If the tumor extends below the superior border of the puborectal sling, sphincter-sparing resection is not feasible (Fig 12) (45).

Pelvic Sidewall

Although pelvic sidewall involvement by tumor is not an absolute contraindication to the surgery, it is essential to alert the surgeons to the presence and degree of sidewall extension so they can determine if resection is feasible and plan ahead for the LEER procedure (Fig 3).

Diagnostic criteria for pelvic sidewall invasion are tumor extending to and abutting the obturator internus or piriformis muscles with associated loss of the intervening fat plane (Fig 13) (23,25). Urogenital diaphragm invasion is similarly defined by involvement of the coccygeus or levator ani muscles. When these standards are applied, MR imaging has a positive predictive value of up to 88% and negative predictive value of up to 97% for the presence of pelvic sidewall extension (23). CT images that show direct contact between FDG-avid tumor and muscles with no intervening fat plane are indicative of pelvic sidewall invasion at FDG PET/CT.

Pelvic Bone Involvement

It is important to define the relation of persistent or recurrent tumor to the adjacent bone to assess

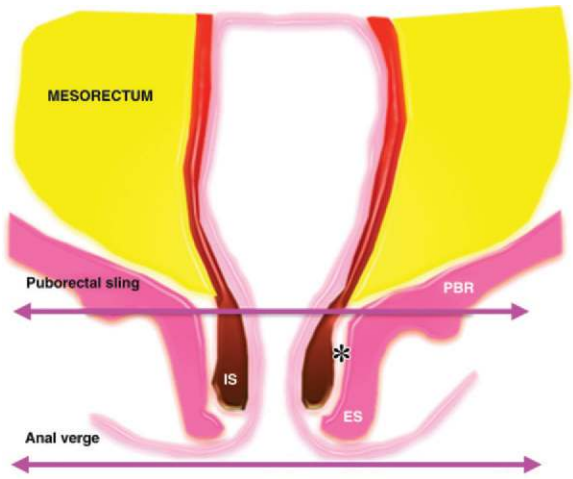

Figure 12. Anatomy of the low rectal region. The internal sphincter *(IS)* is a continuation of the circular muscle layer of the rectum, which thickens at the anorectal junction. The external sphincter *(ES)* complex is an extension of the inferior portions of the levator ani and puborectalis *(PBR)* muscles. If the tumor spreads below the superior border of the puborectal sling, sphincter-sparing resection is not an option. Note that the intersphincteric space (*) is only a few millimeters in width.

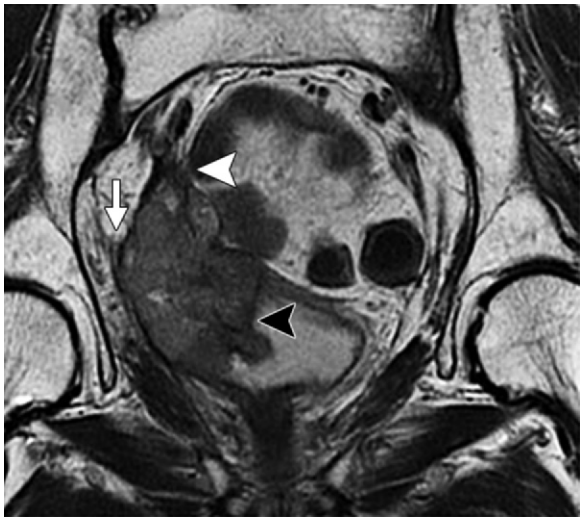

Figure 13. Recurrent endometrial carcinoma in a 69-year-old patient. Coronal FSE T2-weighted image shows a large right pelvic tumor closely abutting the right obturator internus muscle (arrow), invading the urinary bladder (black arrowhead), and abutting the right internal iliac vein (white arrowhead). Note the radiation-related T2 hyperintensity in the right obturator internus muscle.

its resectability and the need for involvement by the orthopedic surgeon. Extended pelvic resection can be combined with standard exenterative techniques to resect the pelvic bones, sacrum, or coccyx affected by the tumor. The radiologist should be aware that upper sacral involvement is generally a contraindication to PE. Some authors consider tumor extension above S1 unresectable, while others believe that tumor invasion above S2 is inoperable (46).

On MR images, bone invasion is suspected when intermediate T2 signal enhancing tumor extends up to the bone with accompanying low signal intensity on T1-weighted images and moderately high signal intensity on fat-saturated T2-weighted images. Loss of a well-defined T1-hypointense band superficial to the bone marrow implies cortical bone destruction (Fig 14). FDG PET/CT is complementary to MR imaging in displaying bone abnormalities. PET can demonstrate metabolically active metastatic disease even before cortical involvement or destruction by tumor is evident at CT (31).

Contraindications to PE

Common or External Iliac Vessel Involvement

Encasement of the common or external iliac vessels is a relative contraindication to exenteration because R0 resection typically cannot be achieved and the prognosis is poor. In a recently published series, only one of five patients with major vascular resection had microscopically negative margins and the entire group had 0% 5-year overall survival (6). On the other hand, internal iliac artery or vein encasement is not an obstacle because, if involved, internal iliac vessels can be sacrificed at the time of LEER (8).

The relationship between the tumor and major vessels is best evaluated on high-resolution multiplanar T2-weighted images. In general there is a paucity of published data on vascular assessment in patients undergoing PE. It is probably safe to assume that a well-defined and uninterrupted fat plane around a vessel excludes vascular involvement. Tumor-vessel contact of 180° is generally considered highly specific for encasement.

Irregular vessel contour including teardrop deformity and change in luminal caliber are signs of vascular involvement regardless of the degree of tumor-vessel contact (Fig 15). Although specific, these criteria are likely not sensitive for detecting vascular invasion. Therefore, the imaging report should also provide information about the presence and degree of contact between the tumor and common or external iliac vessels (Fig 3).

Nerve Involvement

If the tumor involves the lumbosacral plexus or proximal sciatic nerve, the patient may not be a candidate for PE (8). The lumbar plexus is derived from the ventral rami of L1–L4 and is anatomically located behind the psoas muscle (47,48). A minor branch of L4 combines with the ventral ramus of L5 to form the lumbosacral trunk.

The lumbosacral trunk comes down over the sacral ala and combines with the ventral rami of

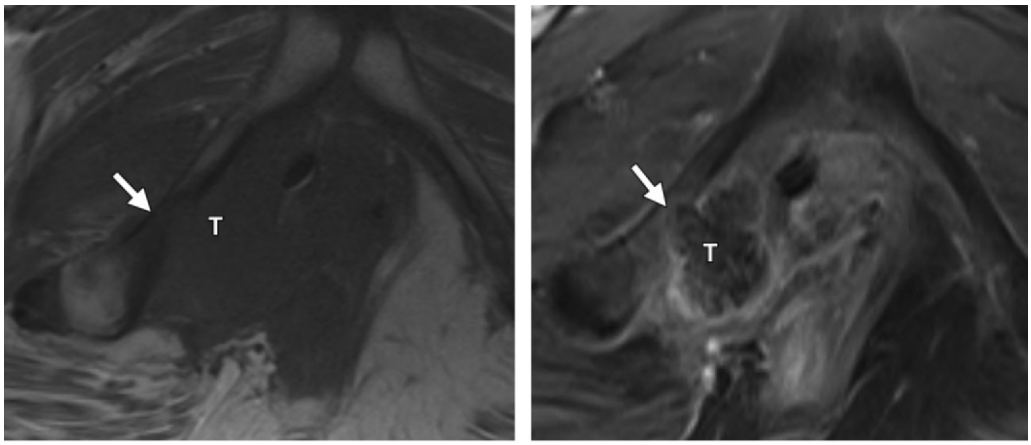

Figure 14. Recurrent pelvic sarcoma in a 55-year-old patient. Axial FSE T1-weighted **(a)** and contrast-enhanced fat-saturated T1-weighted **(b)** images show recurrent tumor *(T)* invading the right inferior pubic ramus (arrow). Bone involvement is evident as loss of the low-signal-intensity cortex and replacement of the normal bone marrow signal by the T1-hypointense tumor, which enhances after intravenous contrast material administration.

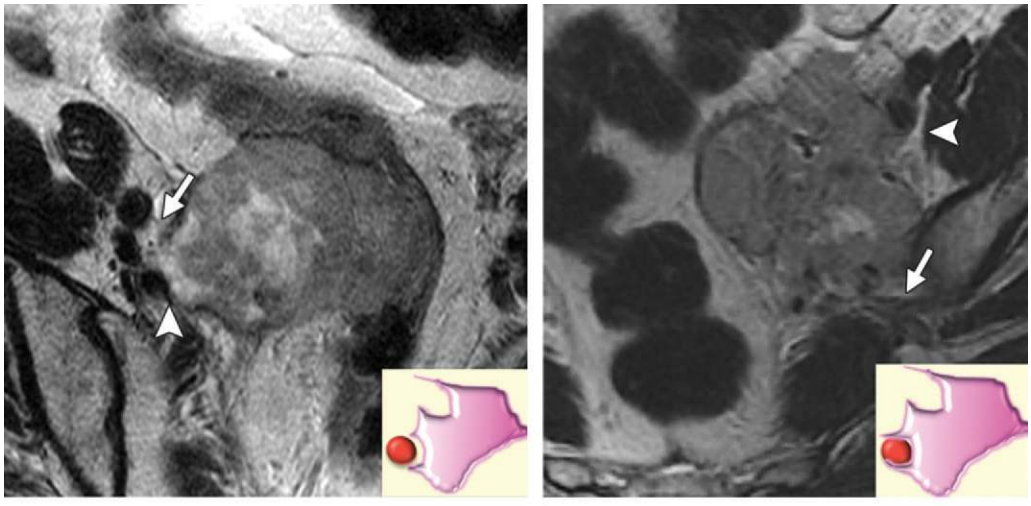

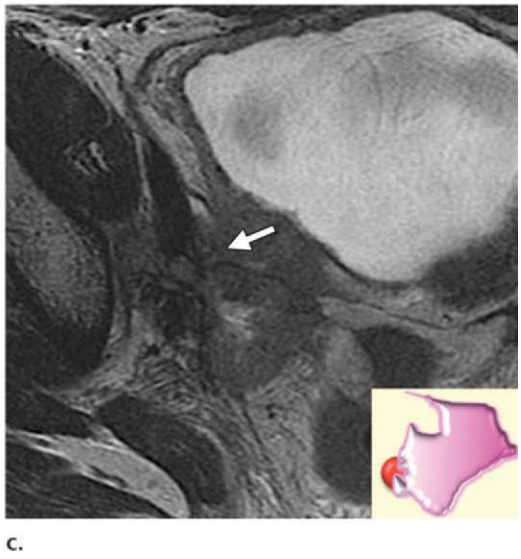

Figure 15. Levels of vascular involvement by tumor. **(a)** Axial FSE T2-weighted image obtained in a 65-year-old patient with recurrent cervical cancer shows a large right pelvic tumor. A fat plane between the tumor and external iliac vessels is preserved (arrow) (inset diagram). Note loss of the fat plane between the tumor and right internal iliac vein (arrowhead). **(b)** Axial FSE T2-weighted image obtained in a 65-year-old woman with recurrent cervical carcinoma shows left pelvic tumor encasing the left external iliac vein (arrowhead) (inset diagram) and approaching the left sciatic nerve (arrow). **(c)** Axial FSE T2-weighted image obtained in a 55-year-old woman with recurrent cervical cancer shows bulky tumor encasing and distorting the external iliac vessels (arrow) (inset diagram).

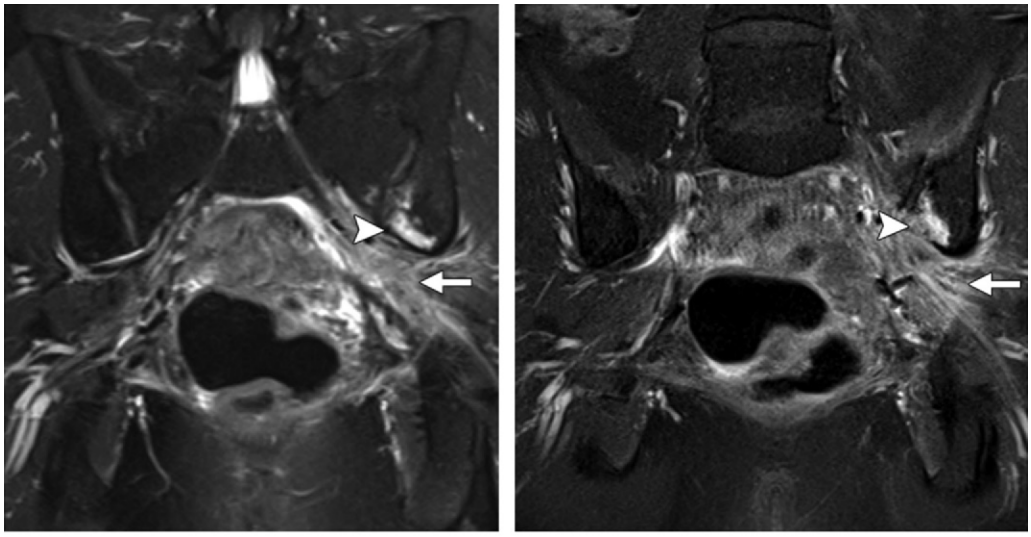

a. b.

Figure 16. Recurrent cervical carcinoma in a 34-year-old patient. Coronal fat-saturated FSE T2-weighted **(a)** and contrast-enhanced fat-saturated T1-weighted **(b)** images show sciatic nerve invasion by the tumor, as evidenced by nerve enlargement, increased T2 signal (arrow in **a**), and presence of contrast enhancement (arrow in **b**). Note the involvement of the adjacent left iliac bone (arrowhead).

S1–S3 (and a branch of S4) to form the sacral plexus (47,48). The individual sacral plexus components are located along the ventral surface of the piriformis muscle, making it a major anatomic landmark for identifying the sacral plexus and sciatic nerve. The sciatic nerve originates from the upper division of the sacral plexus at the lower edge of the piriformis muscle and exits the pelvis through the greater sciatic foramen (47,48).

Although not part of routine evaluation, dedicated MR neurography may be required in patients with clinically suspected lumbosacral plexus or sciatic nerve involvement (47,48). Normal nerve fascicle pattern and preserved fat planes exclude major nerve involvement. Abnormal findings, which should raise suspicion for nerve invasion, include loss of clear fat planes, nerve enlargement (larger than the adjacent artery), increased T2 signal of the nerve (similar to that of adjacent blood vessels), loss of fascicular pattern, and presence of contrast enhancement (Figs 9, 16) (48).

Lymphadenopathy

Some authors believe that both pelvic and extrapelvic metastatic lymph nodes are a contraindication to exenterative surgery. Others think that pelvic lymph node metastases do not preclude curative exenteration (10).

Although no widespread consensus exists regarding the upper limits of normal for lymph node sizes, the general recommendation is to use a short-axis size threshold of 10 mm for retroperitoneal or para-aortic lymph nodes, 8 mm for pelvic lymph nodes, and 15 mm for inguinal lymph nodes (49). Normal lymph nodes typically have a fatty hilum and kidney bean shape. Loss of this typical architecture, rounded contour, and irregular borders should raise suspicion for involvement by tumor (50).

Metastatic lymph nodes may exhibit heterogeneous signal intensity on T2-weighted images and central necrosis on contrast-enhanced images (50). DW imaging can aid nodal detection, since lymph nodes are easily identified as high-signal-intensity ovoid structures (51). Further studies are needed to determine if malignant and benign lymph nodes can be distinguished by measuring their apparent diffusion coefficients (ADCs) (27,52–54).

Both CT and conventional MR imaging have high specificity for detection of nodal enlargement or metastases, but suffer from low sensitivity because normal-sized lymph nodes can frequently harbor metastases (50). By combining functional and structural information, FDG PET/CT has improved sensitivity for identifying metastatic lymph nodes (Fig 17a). For example, it has high sensitivity (75%–100%) and high specificity (87%–100%) for detection of lymph node metastases in patients with advanced-stage cervical cancer (27).

Distant Metastasis

In general patients with distant metastases including peritoneal implants are ineligible for PE (1). Recent data suggests that DW imaging may aid in detection and mapping of peritoneal disease. As the *b* value increases, peritoneal implants remain high signal intensity and become more apparent against the background of suppressed signal from ascites, bowel contents, and fat (27,55,56).

FDG PET/CT is the preferred diagnostic modality for evaluation of suspected systemic

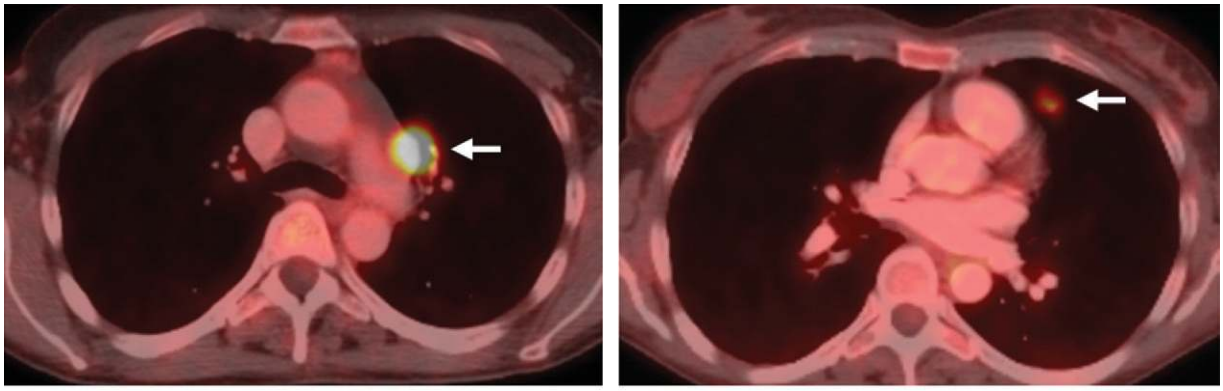

a. b.

Figure 17. Recurrent cervical cancer in a 48-year-old patient. Axial FDG PET/CT images show hypermetabolic thoracic lymphadenopathy (arrow in **a**) and left lung metastasis (arrow in **b**), making this patient ineligible for PE.

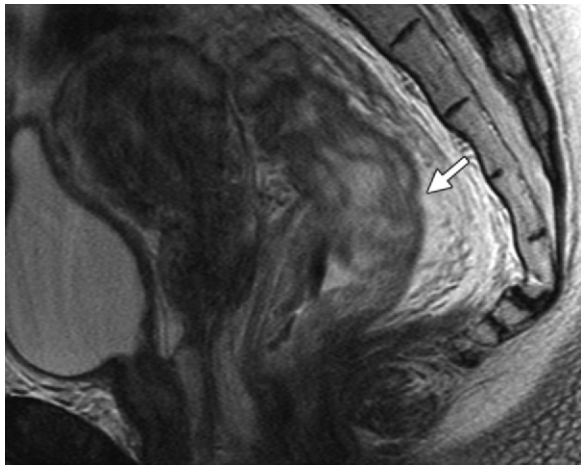

Figure 18. Radiation injury in a 50-year-old patient with cervical carcinoma treated with CRT. Sagittal FSE T2-weighted image shows marked diffuse rectal wall thickening and edema (arrow), consistent with acute radiation-induced proctitis.

metastasis (Fig 17b). A recent meta-analysis found that the pooled sensitivity and specificity of FDG PET or FDG PET/CT for assessment of distant metastasis in recurrent cervical cancer were 87% and 97%, respectively (41).

A recent prospective study conducted in women before PE found that FDG PET had 100% sensitivity and 73% specificity for detection of extrapelvic metastasis (both nodal and systemic metastases) (28). The relatively high rate of false-positive PET findings in that study was attributed to the fact that PET readers were blinded to CT images. Given the potential for false positives, histopathologic confirmation should be obtained before entirely excluding a patient from a potentially curative exenterative procedure (28).

Imaging Pitfalls

Patients being considered for PE have usually undergone various previous treatments including surgery, chemotherapy, and/or radiation therapy. Familiarity with the details of prior management is invaluable to ensure proper context and accuracy of imaging interpretations. Imaging of the irradiated female pelvis is particularly challenging due to the altered normal anatomy, loss of well-defined tissue planes, and radiation-induced injuries to "bystander" organs. When interpreting MR imaging and FDG PET/CT results in women considered for PE, the radiologist should be familiar with the expected imaging appearance of the irradiated pelvis, common posttreatment complications, and modality-specific pitfalls. Although a detailed discussion of this topic is beyond the scope of this review, several key points deserve brief mention.

Pitfalls at MR Imaging

During radiation delivery, adjacent organs inevitably receive a small portion of the total dose directed at the tumor. The likelihood of radiation injury is influenced by the total radiation dose, the volume of irradiated tissue, and concurrent surgery or chemotherapy, which may synergize with and potentiate radiation effects (57).

The urinary bladder is a very radiosensitive organ. At MR imaging, the earliest feature is high T2 signal intensity of the bladder mucosa (bullous mucosal edema) with preserved bladder wall thickness (<5 mm) (Fig 7e) (22). With a more severe injury, the bladder wall becomes thick and demonstrates diffusely increased signal on T2-weighted images (Fig 10). After administration of contrast material, the inflamed mucosa often hyperenhances compared with the rest of the bladder (57). Similarly, increased signal intensity of the rectal submucosa on T2-weighted images is the earliest sign of radiation therapy change. With increased severity of tissue damage, the differentiation between the sub-

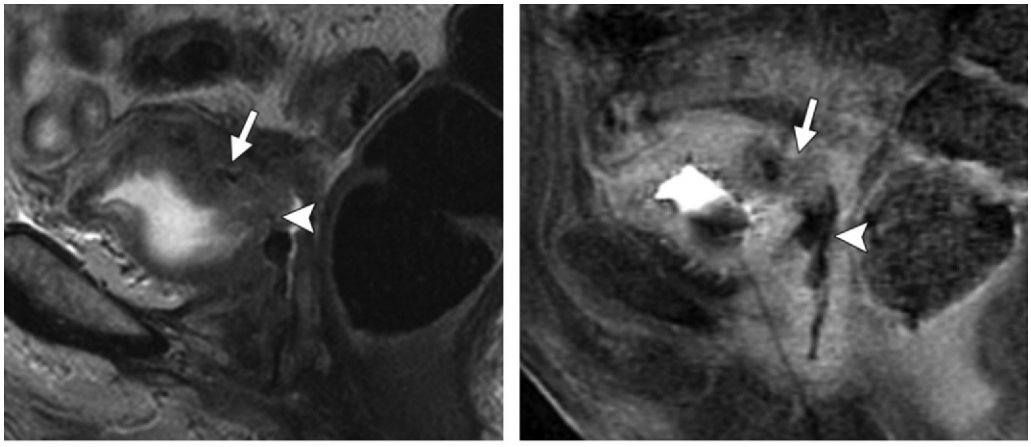

a. b.

Figure 19. Recurrent cervical carcinoma in a 54-year-old patient. Sagittal FSE T2-weighted **(a)** and contrast-enhanced fat-saturated T1-weighted **(b)** images show a recurrent tumor (arrow) with frank posterior bladder wall invasion and secondary vesicovaginal fistula (arrowhead).

mucosa and muscle layer is lost and the rectal wall becomes thick (>6 mm in the distended state) and edematous (Fig 18) (22).

In its most severe form, radiation therapy can cause tissue necrosis leading to fistula formation. Fistulas most commonly occur between the bladder and vagina or between the vagina and rectum. At MR imaging, the sagittal imaging plane is ideal for detection and delineation of fistulas (22). A fistula appears as a linear fluid-filled tract on T2-weighted images and enhances peripherally after contrast material administration (58). It is important to remember that recurrent disease that invades adjacent organs may also be a cause of fistulous tract formation. Therefore, it is essential to evaluate for an associated soft-tissue mass (Figs 7f, 19) (22).

Within a few weeks of radiation therapy bone marrow included in the radiation field acquires relatively uniform high T1 signal intensity due to increased fat content (Fig 20a, 20b) (59). Occasionally during the conversion from hemopoietic to fatty marrow, patchy signal differences may be observed; these should not be confused with bone metastases. Red marrow typically has a feathery appearance because of interspersed fat, whereas tumors do not contain fat and have homogeneous low T1 signal intensity nearly equivalent to that of adjacent skeletal muscles (60).

Fractures of irradiated bones, such as sacral insufficiency fractures and collapsed vertebrae, are relatively common. They may occur within several months after radiation therapy and may mimic osseous metastases. Sacral insufficiency fractures demonstrate a characteristic H-shaped pattern of ill-defined sclerosis in the sacral alae paralleling the sacroiliac joints and extending horizontally across the sacrum (61). This typical pattern can be seen with various imaging modalities including bone scanning, MR imaging, and FDG PET/CT.

At MR imaging, the fracture line demonstrates amorphous or linear foci of decreased signal intensity on T1-weighted images and high-signal-intensity edema around a low-signal-intensity fracture line on T2-weighted images (Fig 20c, 20d) (60). No associated soft-tissue mass is present. In patients with an irradiated pelvis, the H-shaped pattern is consistent with post–radiation therapy pelvic insufficiency fractures even if associated with increased FDG avidity at FDG PET/CT (60,61).

Pitfalls at FDG PET/CT

In oncologic patients, FDG avidity at FDG PET/CT can indicate active disease, but it may also be physiologic in etiology or related to posttreatment inflammation, infection, radiation-induced fistula, or insufficiency fracture. In general it is important to know the patient's relevant menstrual history. In premenopausal women, endometrial FDG uptake can undergo physiologic cyclic variations, increasing during the ovulatory and menstrual phases (31). On the other hand, endometrial FDG avidity is always abnormal in postmenopausal women.

Similarly, although increased ovarian FDG uptake may be functional before menopause, it is associated with malignancy in postmenopausal patients. Furthermore, several benign tumors such as colonic adenomas or uterine leiomyomas may exhibit pronounced FDG avidity (31). False-negative PET findings can occur if the tumor is too small to detect or not metabolically active. The latter consideration is less relevant, since most treatment-resistant gynecologic malignancies considered for PE demonstrate increased glycolytic activity and thus are FDG avid (62).

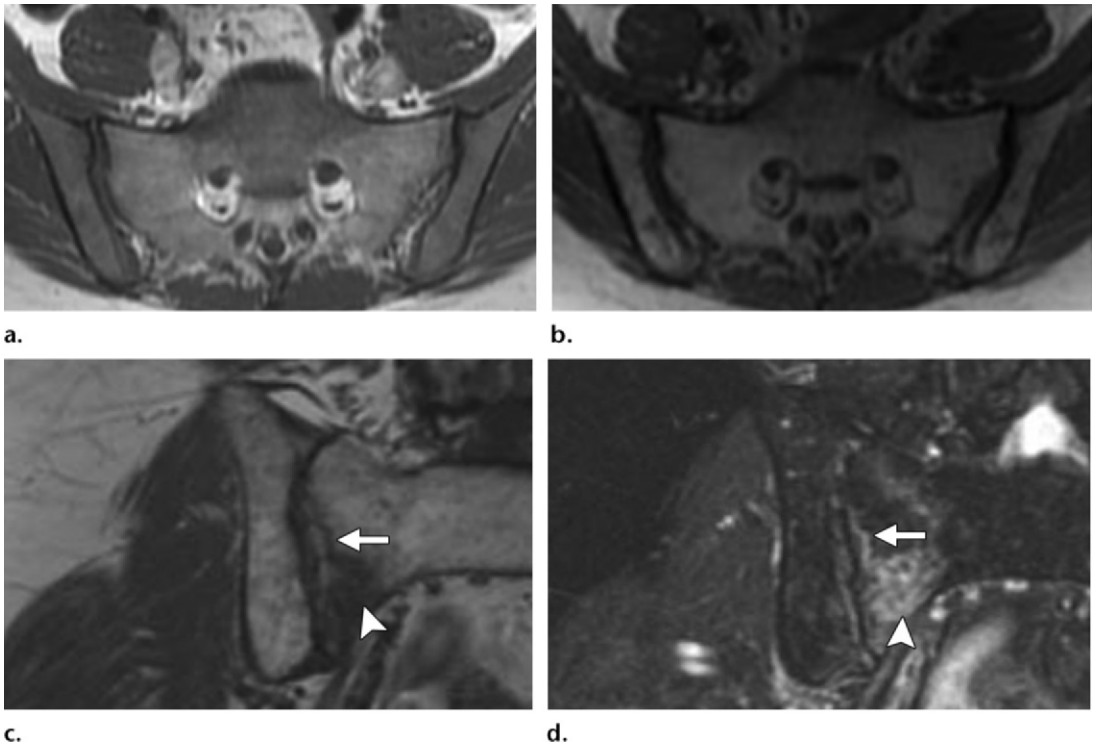

Figure 20. Radiation effects in a 62-year-old patient with cervical carcinoma treated with radiation therapy. **(a, b)** Axial FSE T1-weighted images obtained before **(a)** and after **(b)** radiation therapy show development of diffusely high T1 signal intensity due to radiation-related increased fat content of the bone marrow. One month after completion of radiation therapy, the patient presented to the emergency department with acute-o-nset right hip pain. **(c, d)** Coronal FSE T1-weighted **(c)** and fat-saturated FSE T2-weighted **(d)** images show a T1 hypointense, T2 hyperintense fracture line (arrow), in keeping with an insufficiency fracture. Note the associated edema (arrowhead).

Imaging Evaluation after PE

Normal Imaging Appearance after PE

The normal imaging appearance after PE is highly variable secondary to the variations in the scope of the pelvic resection and types of reconstructive procedures. Familiarity with the exact surgical detail is essential to ensure accurate interpretation of postsurgical imaging studies. In addition, soft-tissue reconstruction of the pelvis increasingly relies on the use of vascularized flaps, including VRAM flaps, omental pedicle flaps, and gracilis myocutaneous flaps. The radiologist should be acquainted with the expected postoperative findings after pelvic reconstruction with these flaps. Complications and disease recurrence are suspected when any deviations from the normal appearance are observed (63).

The omental pedicle flap may be overlooked at cross-sectional imaging, since it has fat attenuation at both CT and MR imaging and may be mistaken for normal pelvic fat (Fig 2c) (9). Since it is composed of fat, the omental pedicle flap does not typically enhance after intravenous contrast material administration. However, it may contain small lymph nodes that should not be misinterpreted as tumor recurrence (13).

The VRAM flap, composed of skin, subcutaneous fat, and a superior portion of the rectus abdominis muscle, is used for pelvic floor or vaginal reconstruction. Postoperatively, the flap is often seen as a unilateral arcuate band of soft tissue extending from the linea alba to the sacrum on either side of the pelvis. The cutaneous portion forms the neovagina, completely encircled by a layer of fat (63). Over time, the muscular part of the VRAM flap usually atrophies due to denervation and is replaced by fat (9).

Bilateral gracilis myocutaneous flaps are perfect for reconstruction of large circumferential vaginal defects resulting from complete vaginectomy (14). During the procedure, the gracilis muscles including overlying skin and subcutaneous fat from the inner aspect of each thigh are dissected, rotated on their neurovascular bundles, and tunneled under the skin into the pelvis to create the neovagina (Fig 2d, 2e) (63). The gracilis muscles may be large in the early postoperative period but frequently atrophy over time. Air in the neovagina is a normal finding (Fig 2e) (64).

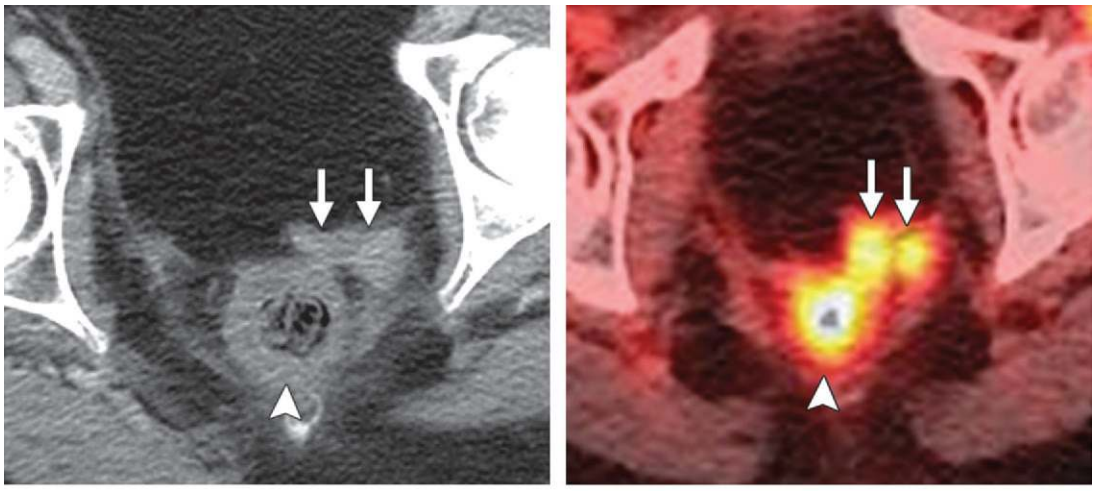

a. b.

Figure 21. Tumor recurrence in a 62-year-old patient after anterior PE for cervical carcinoma recurrence. Axial contrast-enhanced CT **(a)** and FDG PET/CT **(b)** images show two FDG-avid soft tissue nodules (arrows) along the posterior aspect of the omental flap and anterior to the rectum (arrowhead), consistent with recurrent disease.

Complications after PE

PE is one of the most challenging surgical procedures in gynecologic oncology, demanding broad surgical expertise and a multidisciplinary team approach. Factors known to adversely affect operative morbidity are the complexity of pelvic reconstruction and prior radiation therapy leading to impaired healing and immunologic response (17). In the acute postoperative setting, the most common complications seen at imaging are hematoma, abscess, lymphocele, wound dehiscence, colorectal anastomotic insufficiency (abscess, fistula, peritonitis, bowel obstruction), urinary complications (hydronephrosis, urine leak, urinoma, anastomotic breakdown), and myocutaneous flap complications (flap necrosis or abscess; donor site dehiscence, abscess, or seroma) (1).

Late postsurgical complications include anastomotic strictures, fistulas, and tumor recurrence (1,65). Most recurrences occur within 2 years of PE; the majority manifest as a pelvic mass or retroperitoneal or inguinal lymphadenopathy (65). New asymmetric soft tissue or enhancement at CT or MR imaging should be regarded with suspicion (Fig 21a). MR imaging may be better than CT for detection of recurrent disease due to its superior soft-tissue contrast. FDG PET/CT may also help identify disease recurrence by demonstrating hypermetabolic tumor or lymphadenopathy (Fig 21b). Care should be taken to differentiate a recurrent tumor from postsurgical infection or inflammation, which may also be FDG-avid. Although therapeutic options are limited and prognosis is poor, surgical resection may be an option in well-selected patients with small isolated recurrences (65).

Future Perspective

Recent research suggests that fused MR imaging/PET may serve as a predictive biomarker and yield greater diagnostic accuracy and better interobserver agreement than either MR imaging or FDG PET/CT alone (66). With wider adoption and greater availability of hybrid whole-body PET/MR imaging, this novel technique may become a valuable diagnostic tool for patients with treatment-resistant gynecologic malignancies. It may provide a single comprehensive evaluation before PE, alleviating the need for multiple imaging tests.

As this approach evolves, it will be important to determine the patients and pathologic conditions that stand to derive the greatest benefit from PET/MR imaging. Further studies are required to identify the MR imaging sequences most suitable for combining with PET (ie, T2-weighted imaging, DW imaging, or dynamic contrast-enhanced imaging). Finally, as with other costly medical technologies, further studies are needed to establish the cost-benefit and cost-effectiveness of PET/MR imaging.

Conclusion

Over the past 6 decades, considerable modifications in patient selection criteria, surgical techniques, and pelvic reconstruction have transformed PE from a purely palliative approach to a curative surgical procedure. The introduction and validation of MR imaging and FDG PET/CT have noticeably improved pretreatment patient evaluation, thus limiting exenterative surgery (with its associated physical and psychological morbidity) to patients in whom curative resection is possible.

Preoperative MR imaging and FDG PET/CT provide complementary information that aids in detection of extrapelvic disease and allows assessment of local tumor extent. In addition, both modalities synergize to create a preoperative road map for the tailored surgical approach. In the future, whole-body PET/MR imaging may become the imaging technology of choice for women with persistent or recurrent gynecologic cancer before PE.

Acknowledgment.—The authors thank Jennifer Grady, BA, BSN, for her editorial assistance.

References

1. Höckel M, Dornhöfer N. Pelvic exenteration for gynaecological tumours: achievements and unanswered questions. Lancet Oncol 2006;7(10):837–847.
2. Brunschwig A. Complete excision of pelvic viscera for advanced carcinoma. Cancer 1948;1:177–183.
3. Berek JS, Howe C, Lagasse LD, Hacker NF. Pelvic exenteration for recurrent gynecologic malignancy: survival and morbidity analysis of the 45-year experience at UCLA. Gynecol Oncol 2005;99(1):153–159.
4. Baiocchi G, Guimaraes GC, Rosa Oliveira RA, et al. Prognostic factors in pelvic exenteration for gynecological malignancies. Eur J Surg Oncol 2012;38(10):948–954.
5. Diver EJ, Rauh-Hain JA, Del Carmen MG. Total pelvic exenteration for gynecologic malignancies. Int J Surg Oncol 2012;2012:693535.
6. Andikyan V, Khoury-Collado F, Sonoda Y, et al. Extended pelvic resections for recurrent or persistent uterine and cervical malignancies: an update on out of the box surgery. Gynecol Oncol 2012;125(2):404–408.
7. Caceres A, Mourton SM, Bochner BH, et al. Extended pelvic resections for recurrent uterine and cervical cancer: out-of-the-box surgery. Int J Gynecol Cancer 2008;18(5):1139–1144.
8. Höckel M. Laterally extended endopelvic resection (LEER): principles and practice. Gynecol Oncol 2008;111(2 suppl):S13–S17.
9. Sagebiel TL, Faria SC, Balachandran A, Butler CE, Garvey PB, Bhosale PR. Pelvic reconstruction with pedicled thigh flaps: indications, surgical techniques, and postoperative imaging. AJR Am J Roentgenol 2014;202(3):593–601.
10. Pawlik TM, Skibber JM, Rodriguez-Bigas MA. Pelvic exenteration for advanced pelvic malignancies. Ann Surg Oncol 2006;13(5):612–613.
11. Goldberg GL, Sukumvanich P, Einstein MH, Smith HO, Anderson PS, Fields AL. Total pelvic exenteration: the Albert Einstein College of Medicine/Montefiore Medical Center experience (1987 to 2003). Gynecol Oncol 2006;101(2):261–268.
12. Kaufman DS, Shipley WU, Feldman AS. Bladder cancer. Lancet 2009;374(9685):239–249.
13. Mirhashemi R, Averette HE, Estape R, et al. Low colorectal anastomosis after radical pelvic surgery: a risk factor analysis. Am J Obstet Gynecol 2000;183(6):1375–1379; discussion 1379–1380.
14. Pusic AL, Mehrara BJ. Vaginal reconstruction: an algorithm approach to defect classification and flap reconstruction. J Surg Oncol 2006;94(6):515–521.
15. Jurado M, Bazán A, Elejabeitia J, Paloma V, Martínez-Monge R, Alcázar JL. Primary vaginal and pelvic floor reconstruction at the time of pelvic exenteration: a study of morbidity. Gynecol Oncol 2000;77(2):293–297.
16. Kusiak JF, Rosenblum NG. Neovaginal reconstruction after exenteration using an omental flap and split-thickness skin graft. Plast Reconstr Surg 1996;97(4):775–781; discussion 782–783.
17. Chiantera V, Rossi M, De Iaco P, et al. Morbidity after pelvic exenteration for gynecological malignancies: a retrospective multicentric study of 230 patients. Int J Gynecol Cancer 2014;24(1):156–164.
18. Dowdy SC, Mariani A, Cliby WA, et al. Radical pelvic resection and intraoperative radiation therapy for recurrent endometrial cancer: technique and analysis of outcomes. Gynecol Oncol 2006;101(2):280–286.
19. Salom EM, Penalver MA. Pelvic exenteration and reconstruction. Cancer J 2003;9:415–424.
20. Marnitz S, Köhler C, Müller M, Behrens K, Hasenbein K, Schneider A. Indications for primary and secondary exenterations in patients with cervical cancer. Gynecol Oncol 2006;103(3):1023–1030.
21. Morris M, Alvarez RD, Kinney WK, Wilson TO. Treatment of recurrent adenocarcinoma of the endometrium with pelvic exenteration. Gynecol Oncol 1996;60(2):288–291.
22. Addley HC, Vargas HA, Moyle PL, Crawford R, Sala E. Pelvic imaging following chemotherapy and radiation therapy for gynecologic malignancies. RadioGraphics 2010;30(7):1843–1856.
23. Donati OF, Lakhman Y, Sala E, et al. Role of preoperative MR imaging in the evaluation of patients with persistent or recurrent gynaecological malignancies before pelvic exenteration. Eur Radiol 2013;23(10):2906–2915.
24. Kinkel K, Ariche M, Tardivon AA, et al. Differentiation between recurrent tumor and benign conditions after treatment of gynecologic pelvic carcinoma: value of dynamic contrast-enhanced subtraction MR imaging. Radiology 1997;204(1):55–63.
25. Popovich MJ, Hricak H, Sugimura K, Stern JL. The role of MR imaging in determining surgical eligibility for pelvic exenteration. AJR Am J Roentgenol 1993;160(3):525–531.
26. Rockall AG, Ghosh S, Alexander-Sefre F, et al. Can MRI rule out bladder and rectal invasion in cervical cancer to help select patients for limited EUA? Gynecol Oncol 2006;101(2):244–249.
27. Sala E, Rockall AG, Freeman SJ, Mitchell DG, Reinhold C. The added role of MR imaging in treatment stratification of patients with gynecologic malignancies: what the radiologist needs to know. Radiology 2013;266(3):717–740.
28. Husain A, Akhurst T, Larson S, Alektiar K, Barakat RR, Chi DS. A prospective study of the accuracy of 18Fluorodeoxyglucose positron emission tomography (18FDG PET) in identifying sites of metastasis prior to pelvic exenteration. Gynecol Oncol 2007;106(1):177–180.
29. Burger IA, Vargas HA, Donati OF, et al. The value of 18F-FDG PET/CT in recurrent gynecologic malignancies prior to pelvic exenteration. Gynecol Oncol 2013;129(3):586–592.
30. Griffin N, Grant LA, Sala E. Magnetic resonance imaging of vaginal and vulval pathology. Eur Radiol 2008;18(6):1269–1280.
31. Blake MA, Singh A, Setty BN, et al. Pearls and pitfalls in interpretation of abdominal and pelvic PET-CT. RadioGraphics 2006;26(5):1335–1353.
32. Balleyguier C, Sala E, Da Cunha T, et al. Staging of uterine cervical cancer with MRI: guidelines of the European Society of Urogenital Radiology. Eur Radiol 2011;21(5):1102–1110.
33. Flueckiger F, Ebner F, Poschauko H, Tamussino K, Einspieler R, Ranner G. Cervical cancer: serial MR imaging before and after primary radiation therapy—a 2-year follow-up study. Radiology 1992;184(1):89–93.
34. Hricak H, Quivey JM, Campos Z, et al. Carcinoma of the cervix: predictive value of clinical and magnetic resonance (MR) imaging assessment of prognostic factors. Int J Radiat Oncol Biol Phys 1993;27(4):791–801.
35. Hricak H, Swift PS, Campos Z, Quivey JM, Gildengorin V, Göranson H. Irradiation of the cervix uteri: value of unenhanced and contrast-enhanced MR imaging. Radiology 1993;189(2):381–388.
36. Schwarz JK, Siegel BA, Dehdashti F, Grigsby PW. Association of posttherapy positron emission tomography with tumor response and survival in cervical carcinoma. JAMA 2007;298(19):2289–2295.
37. Babar S, Rockall A, Goode A, Shepherd J, Reznek R. Magnetic resonance imaging appearances of recurrent cervical carcinoma. Int J Gynecol Cancer 2007;17(3):637–645.

38. Vincens E, Balleyguier C, Rey A, et al. Accuracy of magnetic resonance imaging in predicting residual disease in patients treated for stage IB2/II cervical carcinoma with chemoradiation therapy: correlation of radiologic findings with surgicopathologic results. Cancer 2008;113(8):2158–2165.
39. Padhani AR, Liu G, Koh DM, et al. Diffusion-weighted magnetic resonance imaging as a cancer biomarker: consensus and recommendations. Neoplasia 2009;11(2):102–125.
40. Meads C, Davenport C, Małysiak S, et al. Evaluating PET-CT in the detection and management of recurrent cervical cancer: systematic reviews of diagnostic accuracy and subjective elicitation. BJOG 2014;121(4):398–407.
41. Chu Y, Zheng A, Wang F, et al. Diagnostic value of 18F-FDG-PET or PET-CT in recurrent cervical cancer: a systematic review and meta-analysis. Nucl Med Commun 2014;35(2):144–150.
42. Magrina JF, Zanagnolo V, Giles D, Noble BN, Kho RM, Magtibay PM. Robotic surgery for endometrial cancer: comparison of perioperative outcomes and recurrence with laparoscopy, vaginal/laparoscopy and laparotomy. Eur J Gynaecol Oncol 2011;32(5):476–480.
43. Sohaib SA, Houghton SL, Meroni R, Rockall AG, Blake P, Reznek RH. Recurrent endometrial cancer: patterns of recurrent disease and assessment of prognosis. Clin Radiol 2007;62(1):28–34; discussion 35–36.
44. Hahn WY, Israel GM, Lee VS. MRI of female urethral and periurethral disorders. AJR Am J Roentgenol 2004;182(3):677–682.
45. Nougaret S, Reinhold C, Mikhael HW, Rouanet P, Bibeau F, Brown G. The use of MR imaging in treatment planning for patients with rectal carcinoma: have you checked the "DISTANCE"? Radiology 2013;268(2):330–344.
46. Kim J. Pelvic exenteration: surgical approaches. J Korean Soc Coloproctol 2012;28(6):286–293.
47. Moore KR, Tsuruda JS, Dailey AT. The value of MR neurography for evaluating extraspinal neuropathic leg pain: a pictorial essay. AJNR Am J Neuroradiol 2001;22(4):786–794.
48. Soldatos T, Andreisek G, Thawait GK, et al. High-resolution 3-T MR neurography of the lumbosacral plexus. RadioGraphics 2013;33(4):967–987.
49. Koh DM, Hughes M, Husband JE. Cross-sectional imaging of nodal metastases in the abdomen and pelvis. Abdom Imaging 2006;31(6):632–643.
50. McMahon CJ, Rofsky NM, Pedrosa I. Lymphatic metastases from pelvic tumors: anatomic classification, characterization, and staging. Radiology 2010;254(1):31–46.
51. Thoeny HC, Triantafyllou M, Birkhaeuser FD, et al. Combined ultrasmall superparamagnetic particles of iron oxide-enhanced and diffusion-weighted magnetic resonance imaging reliably detect pelvic lymph node metastases in normal-sized nodes of bladder and prostate cancer patients. Eur Urol 2009;55(4):761–769.
52. Lin G, Ho KC, Wang JJ, et al. Detection of lymph node metastasis in cervical and uterine cancers by diffusion-weighted magnetic resonance imaging at 3T. J Magn Reson Imaging 2008;28(1):128–135.
53. Kim JK, Kim KA, Park BW, Kim N, Cho KS. Feasibility of diffusion-weighted imaging in the differentiation of metastatic from nonmetastatic lymph nodes: early experience. J Magn Reson Imaging 2008;28(3):714–719.
54. Nakai G, Matsuki M, Inada Y, et al. Detection and evaluation of pelvic lymph nodes in patients with gynecologic malignancies using body diffusion-weighted magnetic resonance imaging. J Comput Assist Tomogr 2008;32(5):764–768.
55. Fujii S, Matsusue E, Kanasaki Y, et al. Detection of peritoneal dissemination in gynecological malignancy: evaluation by diffusion-weighted MR imaging. Eur Radiol 2008;18(1):18–23.
56. Low RN, Gurney J. Diffusion-weighted MRI (DWI) in the oncology patient: value of breathhold DWI compared to unenhanced and gadolinium-enhanced MRI. J Magn Reson Imaging 2007;25(4):848–858.
57. Hricak H. Postoperative and postradiation changes in the pelvis. Magn Reson Q 1990;6(4):276–297.
58. Semelka RC, Hricak H, Kim B, et al. Pelvic fistulas: appearances on MR images. Abdom Imaging 1997;22(1):91–95.
59. Blomlie V, Rofstad EK, Skjønsberg A, Tverå K, Lien HH. Female pelvic bone marrow: serial MR imaging before, during, and after radiation therapy. Radiology 1995;194(2):537–543.
60. Hwang S, Panicek DM. Magnetic resonance imaging of bone marrow in oncology, part 2. Skeletal Radiol 2007;36(11):1017–1027.
61. Ulaner G, Hwang S, Lefkowitz RA, Landa J, Panicek DM. Musculoskeletal tumors and tumor-like conditions: common and avoidable pitfalls at imaging in patients with known or suspected cancer. I. Benign conditions that may mimic malignancy. Int Orthop 2013;37(5):871–876.
62. Lai CH, Lin G, Yen TC, Liu FY. Molecular imaging in the management of gynecologic malignancies. Gynecol Oncol 2014;135(1):156–162.
63. Willing SJ, Pursell SH, Koch SR, Tobin GR. Vaginal reconstruction with rectus abdominis myocutaneous flap: CT findings. AJR Am J Roentgenol 1991;156(5):1001–1004.
64. Epstein DM, Arger PH, LaRossa D, Mintz MC, Coleman BG. CT evaluation of gracilis myocutaneous vaginal reconstruction after pelvic exenteration. AJR Am J Roentgenol 1987;148(6):1143–1146.
65. Mourton SM, Sonoda Y, Abu-Rustum NR, Bochner BH, Barakat RR, Chi DS. Resection of recurrent cervical cancer after total pelvic exenteration. Int J Gynecol Cancer 2007;17(1):137–140.
66. Vargas HA, Burger IA, Donati OF, et al. Magnetic resonance imaging/positron emission tomography provides a roadmap for surgical planning and serves as a predictive biomarker in patients with recurrent gynecological cancers undergoing pelvic exenteration. Int J Gynecol Cancer 2013;23(8):1512–1519.